COMPARISON BETWEEN TWO METHODS FOR CALCULATING THE SOLAR RADIATIVE FLUXES IN TWO-LAYER BROKEN CLOUDINESS (VISIBLE RANGE)

G.A. Titov and T.B. Zhuravleva

Institute of Atmospheric Optics,
Siberian Branch of the Russian Academy of Sciences, Tomsk
Received December 30, 1998
Accepted January 5, 1999

A need to examine the problem of radiative transfer in the two-layer broken cloudiness was repeatedly discussed by us when Georgii Aleksandrovich was alive. I consider it my duty to implement the conceived ideas as a mark of my profound gratitude and respect for Georgii Aleksandrovich – my Teacher, Colleague, and Friend.

Tat'yana Zhuravleva

Mean fluxes of solar radiation at different atmospheric altitude levels are calculated by two methods: (1) approximate method (under assumption of random cloud layer overlap) and (2) method of closed equations based on the Monte Carlo solution of equations for mean intensity in the two-layer broken cloudiness. The calculations have been done for the cloud parameters characteristic of the typical cloud systems (St) – (As), (St) – (Ci), (Cu) – (As), and (Cu) – (Ci) at mid-latitudes of the Northern Hemisphere. It is shown that, depending on the geometrical and optical cloud parameters, the relative difference between the upwelling and downwelling radiative fluxes, calculated by different methods, may reach several tens of percent.

1. INTRODUCTION

Atmospheric cloud layers may simultaneously occur at different altitude levels: two or more cloud layers are usually associated with the passage of atmospheric fronts or decay of massive cumulus or cumulonimbus clouds. The multilayer structure of frontal clouds within the troposphere over the European part of the former USSR was studied by Baranov[1]: the average annual number of cloud layers (being approximately the same for warm and cold seasons) is given in Table I.

The data on multilayer cloud structure over different regions of the former USSR were presented by Dubrovina.[2] A disadvantage of these data is the lack of information concerning upper-level clouds. The low- and medium-level clouds, in accordance with Ref. 2, have a single-layer structure in 30–50% of cases, two-layer structure in about 30% of cases, and three- or four-layer structure in 30% of cases in summer and 20% of cases in winter.

TABLE I. Recurrence (in %) of the number of cloud layers over the European part of the former USSR.[1]

Front	Number of layers				
	1	2	3	4	5 and more
Warm	42.5	37.1	15.3	4.7	0.4
Cold	53	32	12	more than 4 layers – 3	–
Occlusions	40.1	40.2	15	4	0.7

At present there are well-developed methods for calculating radiative effects in horizontally homogeneous multilayer cloudiness (see, for example, Ref. 3). However, when clouds within at least one layer are broken, the radiative characteristics are calculated by approximate methods developed within the framework of the deterministic radiative transfer theory. This circumstance makes them especially attractive for practical implementation, for example, for calculating the short-wave radiative influxes in radiative codes[4–8] of the general atmospheric circulation model (GCM). A significant disadvantage of the given approach is the lack of any estimates of the accuracy of these methods.

0235-6880/99/03 196-08 $02.00

For the Poisson model of broken cloudiness we obtained the equations for the average intensity and developed the Monte Carlo algorithm for calculation of the average solar radiation fluxes in two-layer clouds. The aim of the present paper is to estimate, based on the algorithm proposed here, the accuracy of the approximate method for calculation of the mean fluxes in two-layer broken cloudiness. This will allow the applicability limits of the horizontally homogeneous cloud model to be specified for a class of problems connected with calculations of the energy characteristics of the two-layer cloudiness.

2. THREE-DIMENSIONAL DISTRIBUTION OF CLOUDINESS

To simulate the spatial structure of multilayer cloudiness, we need information on the three-dimensional (3D) cloud distribution, which incorporates at least the following information:

– total cloud fraction and amount of clouds at different altitude levels;

– recurrence of different cloud types and their combinations;

– vertical structure of cloud systems (the number of cloud layers and the altitudes of cloud boundaries).

The State of the art of the studies on climatology of cloud cover has been reviewed in detail in Refs. 9–14. These papers are valuable, because they summarize the results of cloud observations by numerous groups of researchers by means of ground-based network, airborne sensing facilities, and meteorological satellites.

Detailed notion of the *mean total cloudiness*, its variability, and recurrence over the globe for different seasons and latitudes can be inferred from Refs. 2, 9, and 15–18. Marine and continental observational data on *the recurrence of different cloud types* and their combinations have been compiled into special atlases by the American scientists from the Naval Oceanographic Center and National Center for Atmospheric Research. These data compiled for 6 cloud groups (*Ci – Cs – Cc* (*Ci*), *As – Ac* (*As*), *St – Sc* (*St*), *Ns*, *Cu*, and *Cb*) allowed the most typical cloud systems: (*Cu*) – (*As*), (*Cu*) – (*Ci*), (*Cb*) – (*As*), (*Ns*) – (*Cb*), (*St*) – (*Ci*), (*St*) – (*As*), (*Ns*) – (*St*), (*Ns*) – (*As*), and (*As*) – (*Ci*) to be identified.

The above-mentioned data provide fairly complete notion of the statistical characteristics of the global cloud field and are cited in detail in Ref. 19. Also presented there are systematic data on the altitudes of the cloud boundaries and cloud thickness, mostly from the data of airborne sensing.

As to the observational data on *the cloud amount* at different altitude levels, they are scarce and available only for separate regions of the Northern Hemisphere. In general atmospheric circulation models the vertical distributions of cloud amount are calculated from fairly simple empirical formulas, which relate the cloud fraction with the relative humidity in such a way that the calculated average zonal cloud distribution is in agreement with the corresponding realistic distribution. Meleshko[20] proposed a method for calculating the cloud amount at three atmospheric altitude levels starting from the climatic data on the total cloudiness, outgoing radiation at the top of the atmosphere (TOA), temperature, and humidity. The model results agree fairly well with the accumulated empirical data on the vertical distribution of the cloud amount and the main large-scale features of the general atmospheric circulation (GAC). They can be used to calculate the radiative properties of multilayer clouds.

3. MODEL AND CALCULATION TECHNIQUES

3.1. Atmospheric model

The model of the cloudy-aerosol atmosphere is defined in the altitude range $0 \le z \le H_{\text{atm}}^{\text{t}}$ as K separate atmospheric layers (Fig. 1). A unitary flux of solar radiation is incident on the atmospheric upper boundary in the direction $\boldsymbol{\omega}_\odot = (\xi_\odot, \varphi_\odot)$, where $\xi_\odot$ and $\varphi_\odot = 0$ are the solar zenith and azimuth angles.

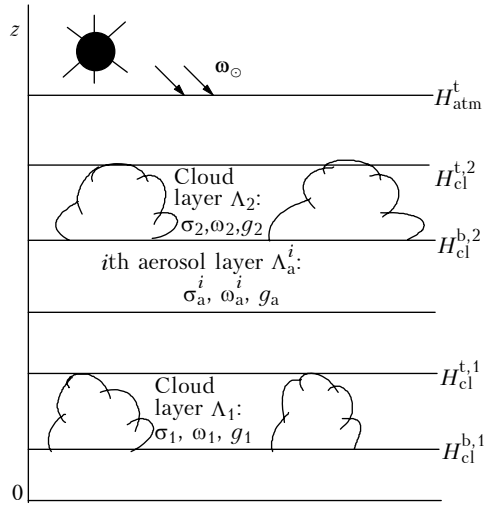

FIG. 1. Schematic illustration of the cloudy-aerosol atmosphere containing two layers of broken cloudiness.

Cloud model. Clouds occupy two separate layers Λ_i, $i = 1, 2$, with the subscripts $i = 1$ corresponding to the lower, and $i = 2$ to the upper layer. Each cloud layer is characterized by the altitudes of its lower boundary (bottom), $H_{\text{cl}}^{\text{b},i}$, and upper boundary (top), $H_{\text{cl}}^{\text{t},i}$: $H_{\text{cl}}^{\text{b},i} \le z \le H_{\text{cl}}^{\text{t},i}$, $i = 1, 2$; $H_{\text{cl}}^{\text{t},1} \le H_{\text{cl}}^{\text{b},2}$.

Within Λ_i the optical model is specified in terms of the random scalar fields of the extinction coefficient $\sigma_{\lambda,i}(\mathbf{r})\ \varkappa_i(\mathbf{r})$, the single scattering albedo $\omega_{\lambda,i}(\mathbf{r})\ \varkappa_i(\mathbf{r})$, and the scattering phase function $g_{\lambda,i}(\boldsymbol{\omega}, \boldsymbol{\omega}', \mathbf{r})\ \varkappa_i(\mathbf{r})$, $i = 1, 2$; the subscript λ stands for the wavelength. The random fields $\varkappa_1(\mathbf{r})$ and $\varkappa_2(\mathbf{r})$

are assumed independent; the mathematical model of $\varkappa_i(\mathbf{r})$, $i = 1, 2$, is constructed with the help of the Poisson point process on the straight lines and is described in detail in Refs. 21 and 22; the optical characteristics within an individual cloud are assumed constant: $\sigma_{\lambda,i}(\mathbf{r}) = \sigma_{\lambda,i}$, $\omega_{\lambda,i}(\mathbf{r}) = \omega_{\lambda,i}$, $g_{\lambda,i}(\boldsymbol{\omega}, \boldsymbol{\omega}', \mathbf{r}) = g_{\lambda,i}(\boldsymbol{\omega}, \boldsymbol{\omega}')$, $i = 1, 2$.

Aerosol model. Each ith aerosol layer Λ_a^i is assumed horizontally homogeneous and is characterized by the extinction coefficient $\sigma_{\lambda,i}^a$, the single scattering albedo $\omega_{\lambda,i}^a$, and the scattering phase function $g_{\lambda,i}^a(\boldsymbol{\omega}, \boldsymbol{\omega}', z)$, $i = 1, 2, \ldots, K$. The vertical stratifications of $\sigma_{\lambda,i}^a$ and $\omega_{\lambda,i}^a$, $i = 1, 2, \ldots, K$, correspond to the mean-cyclic aerosol model[23]; the spectral variability and the vertical profile of $g_{\lambda,i}^a(\boldsymbol{\omega}, \boldsymbol{\omega}', z)$ are not considered. The scattering phase function is calculated in the context of the Mie theory[24] for haze L and the wavelength $\lambda = 0.69$ μm.

The underlying surface reflects the incident radiation according to the Lambert law and has the albedo A_s.

3.2. Method of closed equations

Skorinov and Titov,[25] based on the Poisson model of single-layer broken cloudiness, derived a system of closed equations for the average radiance in statistically homogeneous cloud fields and developed an algorithm for its solution by the Monte Carlo method, referred to as the Method of Closed Equations (MCE). Here, these results are generalized for the *two-layer* broken cloudiness under assumption that the random fields $\varkappa_i(\mathbf{r})$, $i = 1, 2$, are independent and statistically homogeneous.

The problem on the accuracy and applicability limits of the MCE in case of the two-layer clouds, which can be solved by comparison of the results of corresponding numerical simulation, is beyond the scope of our paper. However, we believe that the results obtained for the single-layer broken cloudiness[26] and the hypothesis on independence of random fields $\varkappa_i(\mathbf{r})$, $i = 1, 2$, ensure reasonable accuracy here.

3.3. Approximate calculation technique

The approximate method for calculating a radiative characteristic F (for example, the radiative flux or radiance in a given direction) under conditions of the two-layer broken cloudiness is defined by the formula

$$F = K_{clr=1,\,clr=2}\, F_{clr=1,\,clr=2} + K_{pp=1,\,clr=2}\, F_{pp=1,\,clr=2} + K_{clr=1,\,pp=2}\, F_{clr=1,\,pp=2} + K_{pp=1,\,pp=2}\, F_{pp=1,\,pp=2}. \quad (1)$$

Here, $F_{clr=1,\,clr=2}$, $F_{pp=1,\,clr=2}$, $F_{clr=1,\,pp=2}$, $F_{pp=1,\,pp=2}$ are the clear-sky (clr) and overcast (pp) values of F in single- and two-layer cloudiness, calculated from the deterministic radiative transfer equation. Their weights are specified in accordance with a hypothesis of cloud overlap. Of the three well-known hypotheses – minimum, maximum, and random overlap (see, for example, Ref. 27) – GCM's employ, as a rule, the last two or their combination. A hybrid scheme assumes the application of the hypothesis of maximum overlap for contiguous cloud layers (for example, located at the same altitude level) and the hypothesis of random overlap for non-intersecting layers (for clouds located at different altitude levels). These hypotheses were neither substantiated theoretically nor verified experimentally. They are chosen for each model to fit the results of simulation to the available data of satellite or ground-based observations.[28]

Let N_1 and N_2 be the cloud fractions for the lower and upper cloud layers, respectively. Then the upwelling (downwelling) solar radiative fluxes $F^{\uparrow(\downarrow)}$ at an altitude level z are calculated by the formulas:

for the hypothesis of *random* overlap

$$F_{\text{rand}}^{\uparrow(\downarrow)}(z) = (1 - N_1)(1 - N_2)\, F_{clr=1,\,clr=2}^{\uparrow(\downarrow)}(z) + N_1 (1 - N_2)\, F_{pp=1,\,clr=2}^{\uparrow(\downarrow)}(z) + N_2 (1 - N_1)\, F_{clr=1,\,pp=2}^{\uparrow(\downarrow)}(z) + N_1 N_2\, F_{pp=1,\,pp=2}^{\uparrow(\downarrow)}(z); \quad (2)$$

for the hypothesis of *maximum* overlap

$$F_{\max}^{\uparrow(\downarrow)}(z) = (1 - \max(N_1, N_2))\, F_{clr=1,\,clr=2}^{\uparrow(\downarrow)}(z) + \max(0, N_1 - N_2)\, F_{pp=1,\,clr=2}^{\uparrow(\downarrow)}(z) + \max(0, N_2 - N_1)\, F_{clr=1,\,pp=2}^{\uparrow(\downarrow)}(z) + \min(N_1, N_2)\, F_{pp=1,\,pp=2}^{\uparrow(\downarrow)}(z). \quad (3)$$

4. CALCULATION RESULTS

The mean fluxes in the two-layer broken cloudiness are calculated by the method of closed equations, $F_{\text{MCE}}^{\uparrow(\downarrow)}$, and by the approximate method using the hypothesis on random cloud overlap, $F_{\text{rand}}^{\uparrow(\downarrow)}$. We chose the hypothesis of random overlap, because it is widely used in GCM radiation codes to calculate the radiative fluxes in the presence of clouds at different altitude levels. It is precisely these cloud situations that we consider at the given stage of investigations. The relative difference between the radiative fluxes $F_{\text{MCE}}^{\uparrow(\downarrow)}$ and $F_{\text{rand}}^{\uparrow(\downarrow)}$ will be characterized by the quantity

$$\delta F^{\uparrow(\downarrow)}(z) = 100\% \times \left(F_{\text{rand}}^{\uparrow(\downarrow)}(z) - F_{\text{MCE}}^{\uparrow(\downarrow)}(z)\right) / F_{\text{MCE}}^{\uparrow(\downarrow)}(z).$$

4.1. Cloud parameters

Fluxes of visible solar radiation were calculated for characteristic parameters of typical cloud systems $(St) - (As)$, $(St) - (Ci)$, $(Cu) - (As)$, and $(Cu) - (Ci)$ at mid-latitudes of the Northern Hemisphere[11,19,29,30]:

– optical depth of the lower layer (low-level clouds) varied in the range $10 \le \tau_1 \le 40$, and that of the upper layer (medium- or upper-level clouds) – in the range $1 \le \tau_1 \le 25$;

– scattering phase function of water-drop clouds was calculated using the Mie theory[24] for a wide drop size distribution[29] ($\lambda = 0.69$ μm); the fluxes in ice-crystal clouds were calculated for the scattering phase function of randomly horizontally oriented hexagonal ice crystals[31];

– single scattering albedo $\omega_i = 1$, $i = 1, 2$;

– aspect ratio $\gamma_i = H_i / D_i$ (where H_i and D_i are the thickness and the characteristic horizontal size of cloud elements of the ith cloud layer) in most calculations varied in the range $0 \le \gamma_i \le 2$, $i = 1, 2$. The values of the parameter $\gamma_i \ll 1$ correspond to the cloud formations whose horizontal extent is much greater (at least by an order of magnitude) in comparison with the vertical extent. The values of the parameter $0.5 \le \gamma \le 2$ are typical of the chimney clouds. For the two-layer cloud systems, the value $\gamma = 2$ may be somewhat overestimated for the medium- (*Ac*-type) and upper-level (*Cc*-type) clouds; however, it was used in our calculations to demonstrate the maximum differences which may be obtained for the mean fluxes calculated by two methods;

– height of the atmospheric upper boundary $H^{t}_{atm} = 16$ km;

– underlying surface albedo $A_s = 0$ (which roughly corresponds to the albedo of the ocean).

4.2. Comparison of the calculated results

To better understand the radiative transfer in the two-layer cloudiness, we consider two extreme cases, in which one layer is occupied with the overcast cloudiness and the other – with the broken clouds.

Case 1. Suppose that $N_1 = 1$ and $N_2 < 1$ (the layer of broken cloudiness Λ_2 is over a horizontally homogeneous reflecting surface Λ_1). The approximate method for calculating the solar flux by Eq. (2) is then reduced to the formula

$$F^{\uparrow(\downarrow)}_{rand}(z) = (1 - N_2)\, F^{\uparrow(\downarrow)}_{pp=1,clr=2}(z) + N_2\, F^{\uparrow(\downarrow)}_{pp=1,pp=2}(z). \quad (4)$$

If the reflection from Λ_1 had been described by the Lambertian law, we would have employed the results that have already been obtained (see, for example, Ref. 32). However, the lower cloud layer is non-Lambertian reflector.

Because the optical thickness of the aerosol out of the clouds is small (under the clear-sky conditions, $\tau_a \approx 0.15$), scattering within aerosol layers is negligible in comparison with clouds. Therefore, the solar radiative fluxes, transformed by the two-layer cloudiness, are primarily determined by (a) the unscattered radiation component that passes through gaps between the clouds of the upper layer and reaches the upper boundary of the lower-layer clouds $\Lambda_1 - z = H^{t,1}_{cl}$, and (b) the radiation incident on the top and sides of clouds belonging to the layer.

When the mean upwelling fluxes at the altitude level $z = H^{t,2}_{cl}$ are calculated from formula (4), the contribution of the unscattered radiation component (a) that had passed through the cloud gaps and reached the altitude level $z = H^{t,1}_{cl}$ is described by the first term. In contrast with the MCE, this method makes no allowance for the fact that the radiation component reflected by the lower cloud layer on the one hand, is attenuated by the clouds belonging to the upper layer Λ_2 and on the other hand, represents an additional source of energy that enhances the radiation interaction between the cloud layers. In addition, the MCE is capable of accounting adequately the contribution of the radiation component (b) to the formation of $F^{\uparrow}(H^{t,2}_{cl})$. A part of radiant energy, after a single reflection or multiple reflections from the lower cloud layer, may reach the altitude level $z = H^{t,2}_{cl}$ through the gaps between the clouds and hence exceed the second term of formula (4), which describes the radiation "locked" between the two overcast cloud layers. To understand which of the factors mentioned above is responsible for the difference between $F^{\uparrow}_{rand}(H^{t,2}_{cl})$ and $F^{\uparrow}_{MCE}(H^{t,2}_{cl})$, additional studies are required (in particular, of the angular distributions of the transmitted solar radiation component at the altitude level $z = H^{b,2}_{cl}$ and of the reflected solar radiation component at the altitude level $z = H^{t,1}_{cl}$). At the given stage we restrict ourselves to the quantitative estimate of the quantity $\delta F^{\uparrow(\downarrow)}$.

Now we consider the case of cloudiness with intermediate cloud fractions N_2, because it has been just this case in which the radiative interaction between Λ_1 and Λ_2 may significantly amend the formation of the radiative fluxes.[32] As calculations showed, for $\xi \le 30°$, $10 \le \tau_1 \le 40$, and $1 \le \tau_2 \le 25$ ($\tau = 1$ for ice-crystal clouds and $\tau \ge 4$ for water-drop clouds) the value of $|\delta F^{\uparrow(\downarrow)}|$ at the cloud layer boundaries does not exceed 5% when $\gamma_2 \ll 1$. As γ_2 increases, $|\delta F^{\uparrow}(H^{t,2}_{cl})|$ and $|\delta F^{\downarrow}(H^{b,1}_{cl})|$ remain within the same limits, whereas the relative flux difference for the altitude levels $z = H^{t,1}_{cl}$ and $z = H^{b,2}_{cl}$ somewhat increases with the increase of τ_2 and reaches about – 15% for $\gamma_2 = 2$, $\tau_2 = 25$, and $N_2 = 0.5$.

As the solar zenith angle increases to 75°, $\delta F^{\uparrow}(H^{t,2}_{cl})$ remains below 5–8% while $0 \le \gamma_2 \le 2$ (Fig. 2*a*). The difference between $F^{\downarrow}_{MCE}$ and $F^{\downarrow}_{rand}$ at the lower boundary of the layer Λ_2 increases with γ_2: for example, when $\tau_1 = 40$ and $\tau_2 = 25$, $\delta F^{\downarrow}(H^{b,2}_{cl})$ changes from $\approx -15\%$ for $\gamma_2 << 1$ to $\approx 30\%$ for $\gamma_2 = 2$. The latter is because in chimney-like clouds the portion of the unscattered radiation S and hence the net transmitted radiation component significantly decrease with the increase of ξ, whereas in clouds with the parameter

$\gamma_2 \ll 1$, S changes insignificantly[33] (up to $\xi \approx 80°$). The large values of $\delta F^{\downarrow}(H_{cl}^{b,2})$ lead to the significant difference between $F^{\uparrow}_{MCE}$ and $F^{\uparrow}_{rand}$ at the upper boundary of the layer Λ_1: whereas $\delta F^{\uparrow}(H_{cl}^{t,1}) \approx$ $\approx -15\%$ for $\gamma_2 \ll 1$ and $\tau_2 = 25$, for $\gamma_2 = 2$ it is as large as 40–60%, depending on τ_1 (Fig. 2*b*). When the system of cloud layers is considered as a whole, the difference between the mean upwelling fluxes $F^{\uparrow}_{MCE}$ and $F^{\uparrow}_{rand}$ at the altitude level $z = H_{cl}^{t,2}$ translates into the difference of up to $\approx -20\%$ between $F^{\uparrow}_{MCE}$ and $F^{\uparrow}_{rand}$ at the lower boundary of the layer Λ_1.

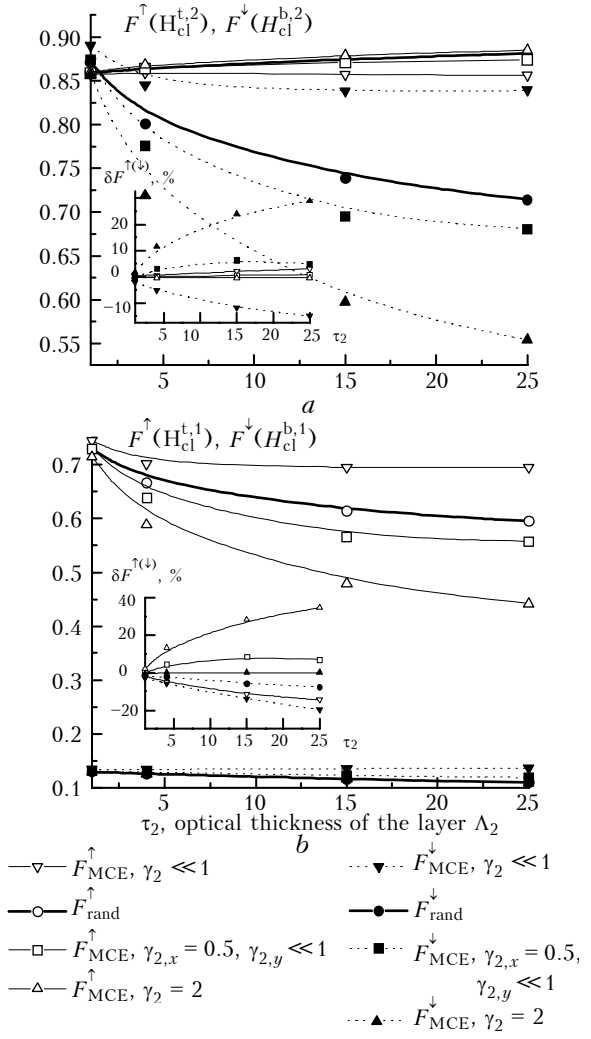

FIG. 2. Mean upwelling and downwelling radiative fluxes and their relative difference $\delta F^{\uparrow(\downarrow)}$ (in %) at the boundaries of (a) the upper Λ_2 and (b) the lower Λ_1 cloud layers for $N_1 = 1.0$, $\tau_1 = 40$, $N_2 = 0.5$, $\xi = 75°$, $A_s = 0$, and different aspect ratios γ_2.

Typically the medium- and upper-level clouds are shaped as bands whose characteristic horizontal extents (D_x along the axis OX and D_y along the axis OY) differ significantly. The calculations made for cloud bands extended along the axis OY ($\gamma_{x,2} = H_2/D_{x,2} = 0.5$, $\gamma_{y,2} = H_2/D_{y,2} \ll 1$) showed that at the boundaries of both cloud layers $|\delta F^{\uparrow(\downarrow)}| \le 10\%$ for the entire range of variation of cloud optical depths (see Fig. 2).

Case 2. Suppose that $N_1 < 1$ and $N_2 = 1$ (the occurrence of the overcast cloud layer Λ_2 over the layer of broken cloudiness is equivalent to the change of the boundary conditions for the underlying cloud layer and transfer from the unidirectional radiation source to the diffuse one).

When the upper layer Λ_2 is optically thin, it is expected that the two methods of mean flux calculations can be compared using the results that had been already obtained in Ref. 33. Let us consider two typical cloud systems, namely, $(St) - (Ci)$ and $(Cu) - (Ci)$. The overcast cirrus cloudiness is quite often encountered: cloud fractions $N \ge 0.8$ were found for *Cs* in 68% of cases in winter and in 44% of cases in summer, whereas for *Cc* and *Ci* clouds this was true in 20% of cases.[30]

For $\gamma_1 \ll 1$ and practically for the entire range of variations of the input model parameters ($10 \le \tau_1 \le 40$ and $\xi \le 75°$) $|\delta F^{\uparrow(\downarrow)}| \le 5\%$, except for $F^{\uparrow}(H_{cl}^{t,1})$. If the lower layer is occupied by cumulus clouds, for small and intermediate cloud fractions the upwelling fluxes at the upper boundary of the layer Λ_2 and at its lower boundary Λ_1 differ stronger: at $\gamma_1 = 2$ $\delta F^{\uparrow}(H_{cl}^{t,2}) \approx$ $\approx -(10 - 15\%)$ and $\delta F^{\downarrow}(H_{cl}^{b,1}) \approx 10 - 30\%$. As γ_1 increases, the relative difference between the mean upwelling fluxes at the altitude level $z = H_{cl}^{t,1}$ changes from $\approx 10-20\%$ to $\approx -25 - 50\%$ for $N_1 \le 0.5$ (Table II).

Now we assume that the upper cloud layer has large optical thickness: $\tau_2 = 25$ (medium-level *As*-type clouds). The upwelling flux at the upper boundary of the two-layer cloudiness is formed by the radiation component scattered only within Λ_2 and by the component participating in the radiative exchange between the cloud layers. As calculations showed, the contribution of the layer Λ_2 itself to $F^{\uparrow}(H_{cl}^{t}2)$ is large: thus, for the parameters indicated in the caption to Fig. 3 it exceeds 90%. As a consequence, the values of $F^{\uparrow}(H_{cl}^{t,2})$, calculated by different methods, agree well practically for the entire range of variation of the input model parameters: $|\delta F^{\uparrow}(H_{cl}^{t,2})| \le 5\%$ (Fig. 3*a*). For intermediate values of the optical thickness $1 < \tau_2 < 25$, the range of variation of $|\delta F^{\uparrow}(H_{cl}^{t,2})|$ is increased up to 10%. The difference between the downwelling fluxes at the lower boundary of the layer is also reasonable: the maximum value of $\delta F^{\downarrow}(H_{cl}^{b,1})$ is $\approx -(10 - 15)\%$.

TABLE II. Radiative fluxes $F^{\uparrow(\downarrow)}_{\rm rand}$ *and* $F^{\uparrow(\downarrow)}_{\rm MCE}$ *and their relative difference* $\delta F^{\uparrow(\downarrow}$ *(shown in parentheses, in %) in the two-layer cloud systems* $(St) - (Ci)$ $(\gamma_1 \ll 1)$ *and* $(Cu) - (Ci)$ $(\gamma_2 = 2)$ *for* $N_2 = 1$, $\tau_2 = 1$, $\tau_1 = 40$, *and* $\xi = 75°$.

z	$F^{\uparrow(\downarrow)}$	$N_1 = 0.1$	$N_1 = 0.3$	$N_1 = 0.5$
$z = H^{\rm t,2}_{\rm cl}$	$F^{\uparrow}_{\rm rand}$	0.439	0.533	0.627
	$F^{\uparrow}_{\rm MCE}$, $(St) - (Ci)$	0.427 (**2.8**)	0.513 (**3.9**)	0.605 (**3.6**)
	$F^{\uparrow}_{\rm MCE}$, $(Cu) - (Ci)$	0.495 (**−11**)	0.621 (**−14**)	0.711 (**−11**)
$z = H^{\rm b,1}_{\rm cl}$	$F^{\downarrow}_{\rm rand}$	0.569	0.472	0.374
	$F^{\downarrow}_{\rm MCE}$, $(St) - (Ci)$	0.584 (**−2.5**)	0.494 (**−4.4**)	0.399 (**−6.2**)
	$F^{\downarrow}_{\rm MCE}$, $(Cu) - (Ci)$	0.509 (**11.8**)	0.378 (**24.9**)	0.285 (**31.2**)
$z = H^{\rm t,1}_{\rm cl}$	$F^{\uparrow}_{\rm rand}$	0.0833	0.201	0.319
	$F^{\uparrow}_{\rm MCE}$, $(St) - (Ci)$	0.0685 (**21.6**)	0.174 (**15.5**)	0.287 (**11.1**)
	$F^{\uparrow}_{\rm MCE}$, $(Cu) - (Ci)$	0.158 (**−47**)	0.313 (**−36**)	0.425 (**−25**)
$z = H^{\rm b,2}_{\rm cl}$	$F^{\downarrow}_{\rm rand}$	0.649	0.672	0.694
	$F^{\downarrow}_{\rm MCE}$, $(St) - (Ci)$	0.646 (**0.1**)	0.665 (**1**)	0.686 (**1.1**)
	$F^{\downarrow}_{\rm MCE}$, $(Cu) - (Ci)$	0.666 (**−2.6**)	0.697 (**−3.6**)	0.716 (**−3.1**)

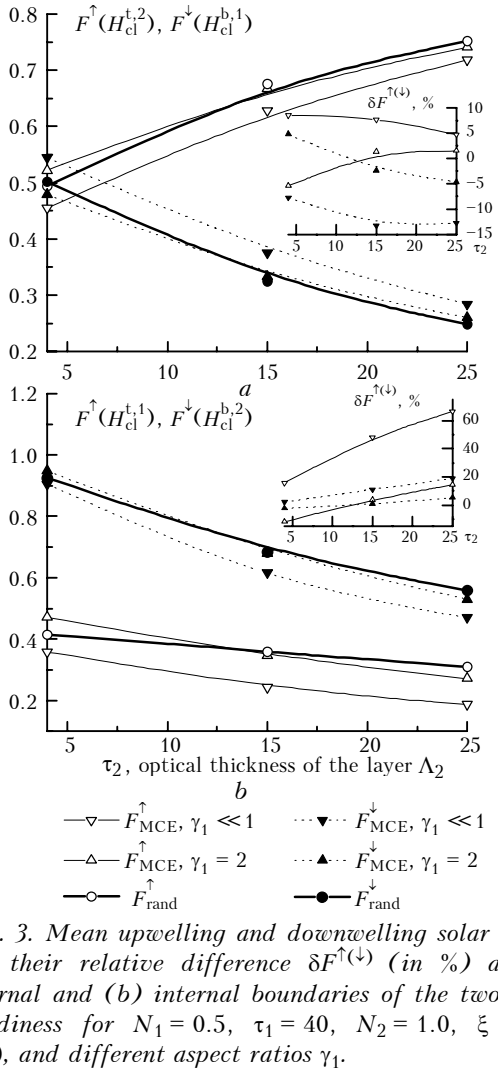

FIG. 3. Mean upwelling and downwelling solar fluxes and their relative difference $\delta F^{\uparrow(\downarrow)}$ *(in %) at (a) external and (b) internal boundaries of the two-layer cloudiness for* $N_1 = 0.5$, $\tau_1 = 40$, $N_2 = 1.0$, $\xi = 30°$, A_s=0, *and different aspect ratios* γ_1.

The relative differences between the fluxes at the internal boundaries of the two-layer cloudiness $z = H^{\rm t,1}_{\rm cl}$ and $z = H^{\rm b,2}_{\rm cl}$ increase up to several tens of percent (Fig. 3*b*) and may reach 100% when the cloud fraction of the lower layer is small and the optical thickness of the layer Λ_2 is large.

We now assume that the upper and lower layers are occupied with partial cloudiness: $N_1 < 1$ and $N_2 < 1$. Calculations were done for cloud fractions N_i, $i = 1, 2$, most typical of the low-, medium-, and high-level clouds for the mid-latitudes of the Northern Hemisphere in summer[20]: 0.3 – 0.5 for low-level clouds and 0.2 – 0.3 for medium- and high-level clouds.

The high-level cloud area is known to exceed 4×10^6 km^2 in almost 30% of cases, but the cloudiness is far from being always overcast.[19] Therefore, it is of interest to compare different methods for calculating the solar fluxes in cloud systems containing cirrus cloudiness, namely, $(St) - (Ci)$ and $(Cu) - (Ci)$.

Now we consider $F^{\uparrow}(H^{\rm t,2}_{\rm cl})$ and $F^{\downarrow}(H^{\rm b,1}_{\rm cl})$ assuming that $0 \le \gamma_1 \le 4$ and $\gamma_2 \ll 1$ (Fig. 4). For the cloud system $(St) - (Ci)$, whose parameters vary in the ranges $10 \le \tau_1 \le 40$ and $30° \le \xi \le 75°$, the relative difference $\delta F^{\uparrow(\downarrow)}$ does not exceed 10%. The increase of the aspect ratio γ_1, that is, transition to the system $(Cu) - (Ci)$, has diverse effects on $\delta F^{\uparrow(\downarrow)}$: whereas for small optical thickness of cumulus clouds ($\tau_1 = 10$) and small solar zenith angles ($\xi = 30°$) $\delta F^{\uparrow(\downarrow)} \le 10\%$, for $\tau_1 = 40$ and $\xi = 75°$, $\delta F^{\uparrow(\downarrow)}$ reaches several tens of percent. Thus, for $\gamma_1 = 2$, $N_1 = 0.5$, and $N_2 = 0.3$, $F^{\uparrow}_{\rm rand}(H^{\rm t,2}_{\rm cl})$ is substantially underestimated in comparison with $F^{\uparrow}_{\rm MCE}(H^{\rm t,2}_{\rm cl})$ [$\delta F^{\uparrow}(H^{\rm t,2}_{\rm cl}) \approx -25\%$], while $F^{\downarrow}_{\rm rand}(H^{\rm b,1}_{\rm cl})$ greatly exceeds $F^{\downarrow}_{\rm MCE}(H^{\rm b,1}_{\rm cl})$ [$\delta F^{\downarrow}(H^{\rm b,1}_{\rm cl}) \approx 60\%$].

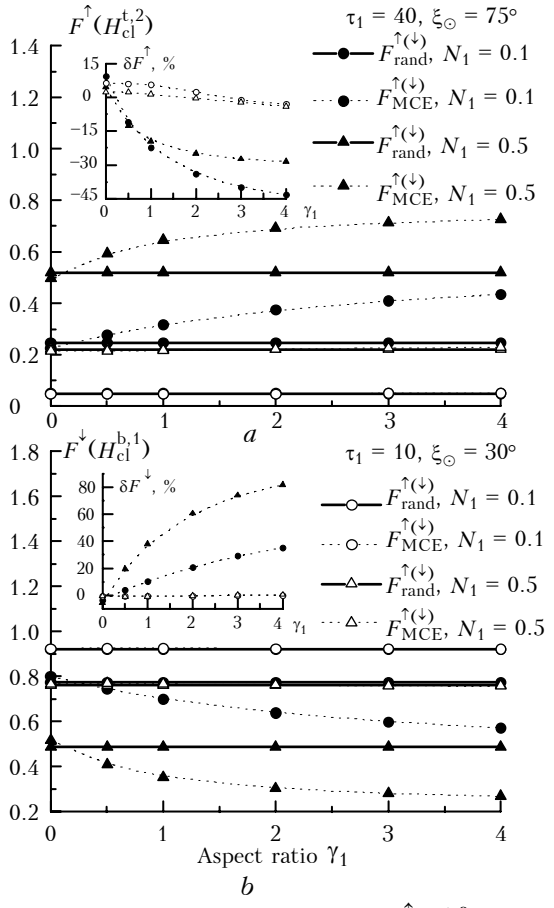

FIG. 4. Dependence of mean fluxes $F^{\uparrow}(H_{cl}^{t,2})$ (a) and $F^{\downarrow}(H_{cl}^{b,1})$ in the cloud system (Cu) – (Ci) on the aspect ratio γ_1 for $\tau_2 = 1$, $N_2 = 0.3$, $\gamma_2 \ll 1$, $A_s = 0$, and different parameters of the lower cloud layer and illumination conditions.

The calculations showed that the variations of the aspect ratio γ_2, i.e., simulation of the upper-level clouds in the form of cloud bands or parallelepipeds, provided that $\gamma_2 \le 2$, did not lead to significant changes of $\delta F^{\uparrow}(H_{cl}^{t,2})$ and $\delta F^{\downarrow}(H_{cl}^{b,1})$ in the cloud systems (St) – (Ci) and (Cu) – (Ci).

Let us compare $F_{MCE}^{\uparrow(\downarrow)}$ and $F_{rand}^{\uparrow(\downarrow)}$ for cloud systems (St) – (As) and (Cu) – (As). We assume that the upper layer is occupied by Ac clouds which, in comparison with As clouds, typically have smaller optical thicknesses. Our choice is because the altocumulus clouds occur during many macroscopic atmospheric processes, so they are quite often encountered in the atmosphere. If the low-level clouds (St or Cu) have relatively small optical thicknesses ($\tau_1 = 10$), then for the solar zenith angles $\xi \le 30°$ and values do not exceed 5%, independent of the value of γ_2 (Fig. 5). As τ_1 and ξ increase, the dependence of $\delta F^{\uparrow}(H_{cl}^{t,2})$ and $\delta F^{\downarrow}(H_{cl}^{b,1})$ on the upper-level cloud field structure, characterized by the aspect ratio γ_2, becomes stronger. For instance, in the system (St) – (As) the increase of γ_2 from 0 to 2 results in the change of $\delta F^{\uparrow}(H_{cl}^{t,2})$ from ≈ 10 to $\approx -10\%$, while $\delta F^{\downarrow}(H_{cl}^{b,1})$ changes from ≈ -10 to $\approx 20\%$. When the layer Λ_1 is occupied by cumulus clouds, the sensitivity of $\delta F^{\uparrow}(H_{cl}^{t,2})$ and $\delta F^{\downarrow}(H_{cl}^{b,1})$ to the upper-level cloud structure decreases; however, the relative difference between the mean fluxes calculated by the approximate method and the MCE increases: for $\gamma_2 = 2$ $\delta F^{\uparrow}(H_{cl}^{t,2})$ reaches $\approx -20\%$, and $\delta F^{\downarrow}(H_{cl}^{b,1})$ reaches $\approx 40 - 50\%$.

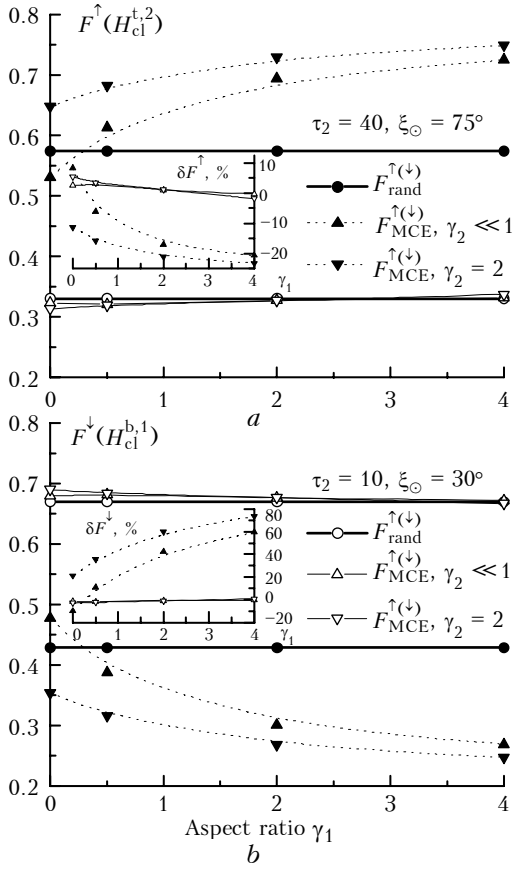

FIG. 5. Dependence of mean fluxes $F^{\uparrow}(H_{cl}^{t,2})$ (a) and $F^{\downarrow}(H_{cl}^{b,1})$ (b) in the cloud system (Cu) – (Ac) on the aspect ratio γ_1 for $\tau_2 = 15$, $N_2 = 0.3$, $N_1 = 0.5$, $A_s = 0$, and different parameters of the lower cloud layer and illumination conditions.

5. CONCLUSION

The mean fluxes of solar radiation in the two-layer broken cloudiness have been calculated using two methods: (1) approximate method (based on the assumption on random cloud overlap) and (2) method of closed equations, based on the Monte Carlo solution of the system of equations for the mean intensity. The MCE not only accounts for the stochastic cloud structure, but also, in comparison with the approximate method, provides more exact description of the radiative interaction between broken cloud layers.

Calculations have been done for the optical-geometric parameters of the cloud systems (St) – (Ci), (St) – (As), (Cu) – (Ci), and (Cu) – (As) and vertical

distributions of the cloud fraction[19,20] typical of the mid-latitudes of the Northern Hemisphere. It has been shown that the relative differences between the upwelling fluxes at the upper boundary of the layer Λ_2 and between the downwelling fluxes at the lower boundary of the layer Λ_1 in the cloud system $(St) - (Ci)$ generally do not exceed 5–10%. When the upper layer is occupied by the water-drop clouds of moderate optical thickness $((St) - (As),\ 4 \le \tau_2 \le 25)$, τ_1 increases from 10 to 40, and ξ increases from 30 to 75°, the values of $|\delta F^{\uparrow}(H_{cl}^{t,2})|$ and $|\delta F^{\downarrow}(H_{cl}^{b,1})|$ may increase up to ≈ 20%. In the cloud systems $(Cu) - (Ci)$ and $(Cu) - (As)$, the mean fluxes $F^{\uparrow}(H_{cl}^{t,2})$ and $F^{\downarrow}(H_{cl}^{b,1})$ depend only weakly on the calculation technique when the optical thickness of the cloud layer Λ_1 is relatively small ($\tau_1 = 10$) and $\xi \le 30°$: $|\delta F^{\uparrow}(H_{cl}^{t,2})|$ and $|\delta F^{\downarrow}(H_{cl}^{b,1})|$ typically are within 5% (rarely amounting to 10%). The larger the optical thickness of the cloud layers and the solar zenith angle, the greater is the difference between the mean fluxes. Thus, the approximate method may underestimate $F^{\uparrow}(H_{cl}^{t,2})$ and overestimate $F^{\downarrow}(H_{cl}^{b,1})$ in comparison with the MCE values by 25–30% and 50–60%, respectively. Depending on the cloud parameters, the relative differences between the fluxes at the levels $z = H_{cl}^{t,1}$ and $z = H_{cl}^{b,2}$ may reach several tens (or even hundreds) percent in all two-layer cloud systems considered here.

REFERENCES

1. A.M. Baranov, *Clouds and Flight Safety* (Gidrometeoizdat, Leningrad, 1983), 231 pp.
2. L.S. Dubrovina, *Clouds and Precipitation from the Data of Airborne Sensing* (Gidrometeoizdat, Leningrad, 1982), 213 pp.
3. J. Lenoble, ed., *Radiative Transfer in Scattering and Absorbing Media. Standard Calculation Techniques* (Gidrometeoizdat, Leningrad, 1990), 263 pp.
4. M. Tiedtke, J.-F. Gelein, A.J. Hollingsworth, and J.F. Louis, Techn. Report ECMWF, No. 10, 1979, 46 pp.
5. A.I. Degtyarev, V.V. Kataev, E.N. Kruglova, L.D. Pogrebenko, and I.V. Trosnikov, Trudy GMT, No. 304, 45–57 (1990).
6. G.P. Kurbatkin, et al., Dokl. Akad. Nauk SSSR **294**, No. 2, 321–324 (1987).
7. V.P. Meleshko, et al., Meteorol. Gidrol., No. 5, 5–14 (1991).
8. V.Ya. Galin, Atmos. Oceanic Opt. **12**, No. 3, 246–250 (1999).
9. L.T. Matveev, ed., *Global Cloud Field* (Gidrometeoizdat, Leningrad, 1986), 279 pp.
10. V.I. Vorob'ev and V.S. Fadeev, *Cloud Cover Parameters for the Northern Hemisphere from the Data of Meteorological Satellites* (Gidrometeoizdat, Leningrad, 1981), 172 pp.
11. K.Ya. Kondratiev and V.I. Binenko, *Cloud Effect on Radiation and Climate* (Gidrometeoizdat, Leningrad, 1984), 240 pp.
12. G.I. Marchuk, K.Ya. Kondratiev, V.V. Kozoderov, and V.I. Khvorost'anov, *Clouds and Climate* (Gidrometeoizdat, Leningrad, 1986), 512 pp.
13. T.G. Berlyand and L.A. Strokina, Trudy Gl. Geofiz. Obs., No. 388 (1974).
14. N.A. Hughes, J. Climate Appl. Meteorol. **23**, 724–751 (1984).
15. T.G. Berlyand, L.A. Strokina, and L.E. Greshnikova, Meteorol. Gidrol., No. 3, 15–23 (1980).
16. T.G. Berlyand and L.A. Strokina, *Global Distribution of Total Cloud Amount* (Gidrometeoizdat, Leningrad, 1980), 71 pp.
17. O.A. Avaste, O.Yu. Kyarner, and C.Kh. Keevalik, Meteorol. Gidrol., No. 7, 54–60 (1981).
18. L.T. Matveev, *Cloud Dynamics* (Gidrometeoizdat, Leningrad, 1980), 311 pp.
19. *Handbook on Clouds and the Cloudy Atmosphere* (Gidrometeoizdat, Leningrad, 1989), 647 pp.
20. V.P. Meleshko, Meteorol. Gidrol., No. 9, 12–23 (1980).
21. G.A. Titov, Izv. Akad. Nauk SSSR, Ser. Fiz. Atmos. Okeana **29**, No. 9, 940–948 (1985).
22. G.A. Titov, J. Atmos. Sci. **47**, 24–38 (1990).
23. V.E. Zuev and G.M. Krekov, *Optical Models of the Atmosphere* (Gidrometeoizdat, Leningrad, 1986), 256 pp.
24. D. Deirmendjian, *Electromagnetic Scattering on Spherical Polydispersions* (American Elsevier Publishing Company, Inc., 1969), 292 pp.
25. V.N. Skorinov and G.A. Titov, in: *Methods and Algorithms for Statistical Simulation* (Computer Center of the Siberian Branch of the USSR Academy of Sciences, Novosibirsk, 1983), pp. 91–99.
26. V.N. Skorinov and G.A. Titov, Izv. Vyssh. Uchebn. Zaved., Ser. Radiofizika **26**, No. 8, 971–980 (1983).
27. J.-J. Morcrette and Y. Fouquart, J. Atmos. Sci. **43**, No. 4, 321–328 (1986).
28. I.I. Mokhov, O.P. Skrotskaya, and I.G. Ostapenko, Izv. Akad. Nauk, Ser. Fiz. Atmos. Okeana **30**, No. 4, 558–563 (1994).
29. E.M. Feigel'son, ed., *Radiation in the Cloudy Atmosphere* (Gidrometeoizdat, Leningrad, 1981), 280 pp.
30. E.M. Feigel'son, ed., *Radiative Properties of Cirrus Clouds* (Nauka, Moscow, 1989), 224 pp.
31. Y. Takano and Kuo-Nan Liou, J. Atmos. Sci. No. 1, 3–19 (1989).
32. G.A. Titov and E.I. Kas'yanov, Atm. Opt. **3**, No. 10, 1108–1114 (1990).
33. V.N. Skorinov and G.A. Titov, Izv. Akad. Nauk SSSR, Ser. Fiz. Atmos. Okeana 20, No. 3, 263–270 (1984).